SEMARAK ILMU PUBLISHING

CFD Letters

Journal homepage:
https://semarakilmu.com.my/journals/index.php/CFD_Letters/index
ISSN: 2180-1363

A Computational Solution of Melting Process inside a Sphere Towards the Latent Heat Storage in a Solar Air Heater

Tran Van Hung[1,2], Tu Thien Ngo[3], Nguyen Minh Phu[4,*]

[1] Faculty of Mechanical engineering, Ho Chi Minh City University of Technology (HCMUT), 268 Ly Thuong Kiet, District 10, Ho Chi Minh City, Vietnam
[2] Vietnam National University Ho Chi Minh City (VNU-HCM), Linh Trung Ward, Thu Duc City, Ho Chi Minh City, Vietnam
[3] Jeong-Woo Industrial Machine Co., Ltd., 253,5 Sandan-ro, Susin-myeon, Dongnam-gu, Cheonan-si 31251, Republic of Korea
[4] Faculty of Heat and Refrigeration Engineering, Industrial University of Ho Chi Minh City (IUH), 12 Nguyen Van Bao, Go Vap District, Ho Chi Minh City, Vietnam

ARTICLE INFO

Article history:
Received 4 August 2024
Received in revised form 8 September 2024
Accepted 12 October 2024
Available online 31 January 2025

Keywords:
Enthalpy method; spherical coordinate; melting fraction; paraffin waxes; energy storage

ABSTRACT

Latent heat storage using the phase change material (PCM) in a solar air collector is a measure to extend the collector's operating time during off sunshine period because air cannot store heat. In this paper, the melting prediction of spherical PCM under hot air convection is established by a one-dimensional unsteady enthalpy equation and solved by the finite difference method. The numerical results are compared with published data to confirm the accuracy. The independent parameters to investigate the charging include sphere diameter, air temperature, air velocity and initial temperature of PCM. The effects of air temperature and sphere diameter are significant on the melting rate of PCM. When the diameter increases by 2.5 times, the time to complete liquefaction increases by 5 times. At an air temperature of 70°C, the required liquefaction time is 75 mins for a 40 mm diameter sphere.

1. Introduction

Solar energy and thermal storage are key components in creating a more efficient and reliable renewable energy system [1]. Solar energy is harnessed using two main types of technology. First, photovoltaic (PV) cells convert sunlight directly into electricity using semiconductor materials. Photovoltaic cells are commonly used in solar panels installed on rooftops or in large solar farms [2]. Second, the solar thermal system collects heat from the sun using collectors, which then heats a material [3,4]. This thermal energy can be used directly for heating or to generate steam to drive turbines to generate electricity [5]. Thermal storage systems are designed to store heat for later use, helping to balance energy supply and demand. Sensible heat storage involves heating a material and storing that thermal energy in the material itself. For example, a tank of water or rocks can store sensible heat. When needed, the stored heat is transferred back to the liquid or air in the system. Latent heat storage uses phase change materials (PCMs) that absorb or release heat during a phase

* *Corresponding author.*
E-mail address: nguyenminhphu@iuh.edu.vn (Nguyen Minh Phu)

https://doi.org/10.37934/cfdl.17.7.6173

change (e.g., from solid to liquid or vice versa) [6,7]. These materials store and release energy more efficiently than sensible heat storage [8].

Combining solar energy with a thermal storage system offers several advantages. Solar energy can be intermittent, so thermal storage helps balance supply by storing excess heat during sunny periods and releasing it when there is no sunlight. Thermal storage allows energy use to be shifted to times when there is no solar energy, thereby reducing dependence on fossil fuels and increasing grid stability [9]. For solar air heaters, since heat cannot be stored in the air, a different medium is needed [10,11]. Research on indirect latent thermal storage, Román *et al.,* [12] stored latent heat in PCM slabs integrated with a solar air heater to dry wheat. As the hot air passes through the air gaps between the PCM slabs, it transfers heat to the PCM. The PCM absorbs this thermal energy and melts, storing the heat in the form of latent heat. When the temperature drops, the stored latent heat can be released, supplying energy back to the drying system. They found that the moisture content was significantly uniform. Yadav *et al.,* [13] accumulated latent thermal energy outside tubes of a solar air collector system for a drying application. Solar energy heats the air using a V-shaped absorber plate under a transparent glass cover. The heated air flows through a thermal energy storage device, storing thermal energy for continuous operation and moves into the drying chamber. The system is designed to work efficiently during sunny periods and continues drying with the stored heat during periods without direct sunlight, allowing for continuous drying. They deduced that the drying process was continued up to 22:00 without an extra heat source. Research on direct latent thermal storage inside spherical PCM, Bouadila *et al.,* [14,15] experimentally examined the latent heat storage in spherical capsules. The capsules were placed below the glass cover and contacted the absorber plate of the air collector. A similar configuration was also investigated by Arfaoui *et al.,* [16] and Sudhakar *et al.,* [17]. The design involves placing stainless steel balls filled with PCM into the holes of the absorber plate. This arrangement allows a portion of the surface of the PCM-filled balls to also contact the bottom plate. This contact between the PCM and the bottom plate slightly increases the heat transfer area, thereby enhancing the thermal conductivity of the collector. Table 1 summarized the researched patterns on direct latent storage and indirect latent storage associated with an air collector.

The above literature review implies that the thermal storage characteristics of PCM sphere under forced convection of air in solar air heater system have not been found. There are many other studies on phase change spheres. However, the studies focus on developing mathematical models and analysing the flow and profile of PCM. In addition, the former simulation researches set wall temperature higher than melting temperature that leaded to phase change as soon as beginning the simulation. This study aims to establish a simplified mathematical model that can be verified and applied in indirect solar thermal energy storage. Indirect storage allows for greater flexibility in system configuration. It can be tailored to different applications and can be easily integrated with existing heating systems or renewable energy sources. By isolating the storage medium from direct exposure to solar radiation, indirect systems can prolong the lifespan of the storage materials, reducing maintenance and replacement costs. Therefore, the present study aims to bridge the relevant data gap. A PCM sphere is placed in hot air flow to receive forced convection heat. The present numerical study is conducted to analyse the influence of geometrical and thermohydraulic parameters on temperature distribution, phase and melting of spherical PCM.

Table 1
Summary of indirect and direct latent thermal storages in solar air heaters

No.	Configuration	Comment	Reference
1	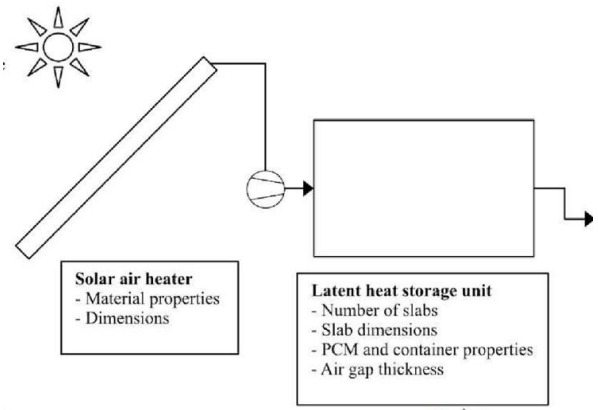	Indirect storage in PCM slabs	[12]
2	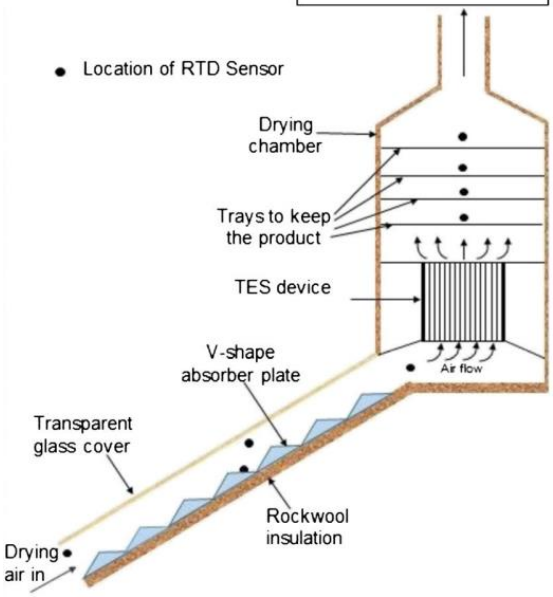	Indirect storage outside tubes	[13]
3	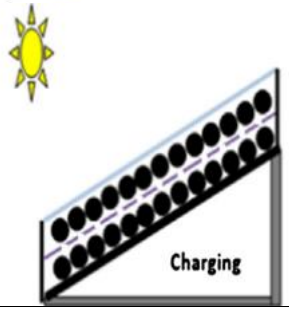	Direct storage in PCM spheres	[14-17]

2. Mathematical Formulation

Figure 1 shows the solar air collector with indirect latent heat storage in the spheres. Air flows through the gap between the glass cover and the absorber plate of the collector to raise temperature. The high-temperature air transfers heat to PCM in the sphere to store heat. This stored heat is used during periods of intermittent sunshine or when the sun is out. Modelling of heat storage in the sphere due to forced convection of the hot air flow is shown in Figure 2.

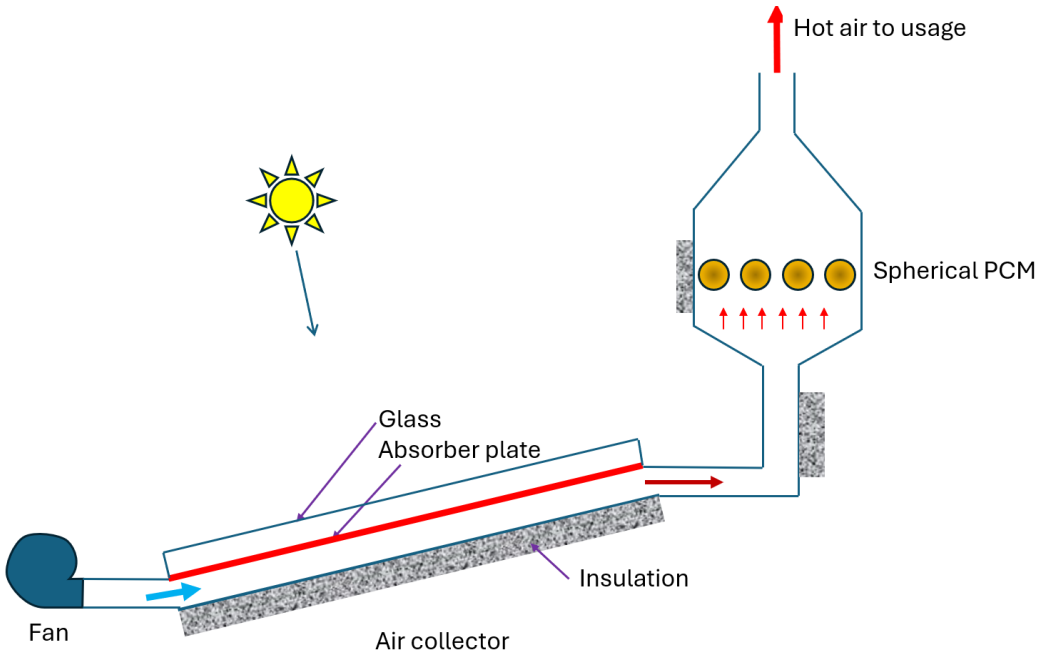

Fig. 1. Solar air heater with indirect latent heat storage inside PCM spheres

A free air stream with velocity u_∞ and temperature T_∞ is blowing to the PCM sphere. The sphere with diameter D has an initial temperature T_{ini} which is less than T_∞ and its melting temperature (T_m), while the temperature $T_\infty > T_m$. The mathematical model is established with the following assumptions:

i. The temperature of the PCM is assumed to vary with time t and radius r, i.e., $T = T(t, r)$.
ii. The thermophysical properties of the PCM are constants.
iii. The convective heat transfer on the sphere surface is uniform.
iv. The distance between the two spheres is far enough to model a single sphere.
v. Natural convection of liquid PCM is neglected.

The melting of the PCM is governed by the following energy equation:

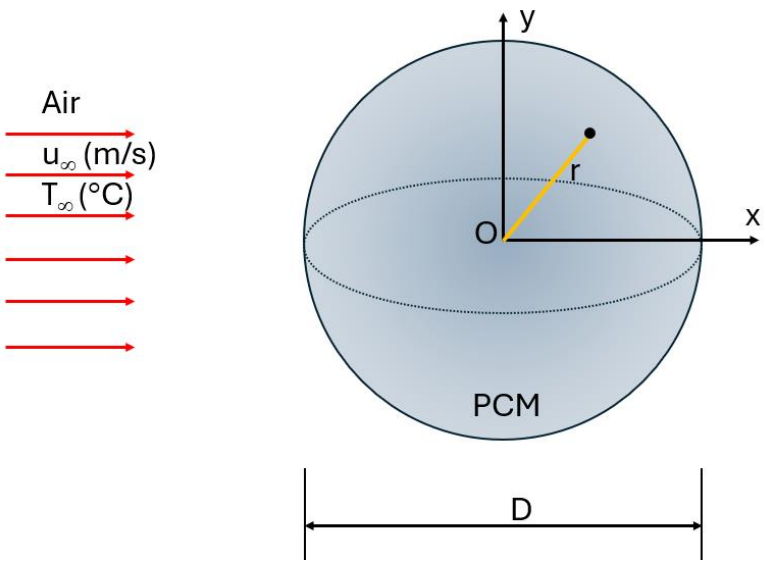

Fig. 2. Modelling of a PCM sphere

$$\frac{\rho_p}{k_p}\frac{\partial H}{\partial t} = \frac{1}{r^2}\frac{\partial}{\partial r}\left(r^2\frac{\partial T}{\partial r}\right) \quad (1)$$

where H is enthalpy, k_p and ρ_p refers to conductivity and density of PCM, respectively.

The phase change of PCM can be estimated by the following enthalpy method [18]:

$$T = \frac{H}{c_{p,p_m}} \quad \text{for } H \leq 0 \quad \text{(solid phase)} \quad (2)$$

$$T = T_m \quad \text{for } 0 < H < L \quad \text{(phase change)} \quad (3)$$

$$T = \frac{H-L}{c_{p,p_m}} \quad \text{for } H \geq L \quad \text{(liquid phase)} \quad (4)$$

where $c_{p,p}$ and L are respectively specific heat and latent heat of fusion of PCM.

The boundary condition at the sphere surface and centre can be expressed as follows. The sphere surface ($r = D/2$) was exposed to the convection boundary condition and symmetry boundary condition was set for the centre ($r = 0$).

$$-k_p \left.\frac{\partial T}{\partial r}\right|_{r=D/2} = h(T|_{r=D/2} - T_\infty) \quad (5)$$

$$\left.\frac{\partial T}{\partial r}\right|_{r=0} = 0 \quad (6)$$

where h is convection heat transfer coefficient of air over a sphere.

The governing equation and boundary conditions were discretized by the explicit finite difference method. Forward time was applied to the unsteady term and central difference to the remaining terms of the energy equation.

$$\frac{\rho_p}{k_p}\frac{H_{i,j}^{n+1} - H_{i,j}^n}{\Delta t} = \frac{T_{i+1,j}^n - 2T_{i,j}^n + T_{i-1,j}^n}{\Delta r^2} + \frac{2}{r}\left(\frac{T_{i+1,j}^n - T_{i-1,j}^n}{2\Delta r}\right) \quad (7)$$

$$-k_p \frac{T_{r=D/2} - T_{r=D/2-\Delta r}}{\Delta r} = h(T|_{r=D/2} - T_\infty) \quad (8)$$

$$T_{r=0} = T_{r=\Delta r} \quad (9)$$

The convection heat transfer coefficient of air over a sphere was determined using the comprehensive correlation of Whitaker [19]:

$$h = \left[2 + \left(0.4Re^{0.5} + 0.06Re^{2/3}\right)Pr^{0.4}\left(\frac{\mu}{\mu_w}\right)^{0.25}\right]\frac{k}{D} \quad (10)$$

where *k*, Pr and μ are respectively thermal conductivity, Prandtl number and dynamic viscosity of air. μ_w is the viscosity of air at the temperature of sphere surface.

It is wished the local convective heat transfer coefficients along the surface of the sphere. However, there is no readily available correlation for doing this. Studies on heat transfer during drying of spheres have also taken a constant heat transfer coefficient and have shown reasonable results [20-22]. Whitaker's equation is applicable to flow around spheres and packed beds with a wide range of applications ($3.5 \leq Re \leq 7.6\times10^4$, $0.71 \leq Pr \leq 380$ and $1.0 \leq \mu/\mu_s \leq 3.2$) [23].

The Reynolds number of air (Re) is evaluated as:

$$Re = \frac{\rho D u_\infty}{\mu} \tag{11}$$

where ρ is the density of air.

The thermophysical properties of air as functions of temperature (from 50 to 100°C) at atmospheric pressure were extracted from the EES software as Klein [24]:

$$\mu = 0.0000173114207 + 4.79697859 \times 10^{-8} \cdot T_\infty - 2.99428526 \times 10^{-11} \cdot {T_\infty}^2 \tag{12}$$

$$Pr = 0.734788989 - 0.000275345913 \cdot T_\infty + 4.63928196 \times 10^{-7} \cdot {T_\infty}^2 \tag{13}$$

$$\rho = 1.2804365 - 0.00418449417 \cdot T_\infty + 0.00000840883479 \cdot {T_\infty}^2 \tag{14}$$

$$k = 0.0237667766 + 0.0000719213027 \cdot T_\infty \tag{15}$$

In the current work, properties of paraffin wax as a PCM have the values as: specific heat $c_{p,p}$ = 2000 J/kg K [12], conductivity k_p = 0.2 W/m K, density ρ_p = 750 kg/m^3 [25], melting temperature T_m = 49°C [13] and latent heat of fusion $L = 1.9\times10^5$ J/kg [12]. It should be noted that there are some kinds of paraffin wax such as RT-47, RT-50 and RT-60. But their properties are mostly the same. The phase changes with a long period are unaffected by the properties as pointed out experimentally and numerically by Ismail *et al.*, [26].

Finite difference formulation is programmed in Matlab R2016a language [27] with the stability condition as follows [28]:

$$\frac{k_p}{c_{p,p}\rho_p}\frac{\Delta t}{\Delta r^2} \leq \frac{1}{2} \tag{16}$$

The time step was chosen to be Δt = 0.5 s. From the independent grid checks with different spatial steps Δr, the results show that Δr = 0.4 mm ensured grid-independent solution and moderate calculation time. Figure 3 shows a comparison of the calculated results in this study with published results. In this comparison, the sphere has a diameter of D = 100 mm and ΔT = 15°C is the temperature difference between the sphere surface and the melting. Liquid fraction is the ratio of volume of the liquid to the volume of the sphere. There is good agreement between the two results, especially for the first 25 minutes. Furthermore, after 350 minutes of heating the PCM, all the PCM in the sphere melted into liquid, i.e., liquid fraction equals unity, which demonstrates an absolute match between the two results. The liquid phase fraction obtained in this study is consistently lower

than that reported in the study of Ismail *et al.*, [26] at the same time points. This is due to the fact that a limitation of the current study is the omission of natural convection in liquid PCM, which can influence the rate of phase change.

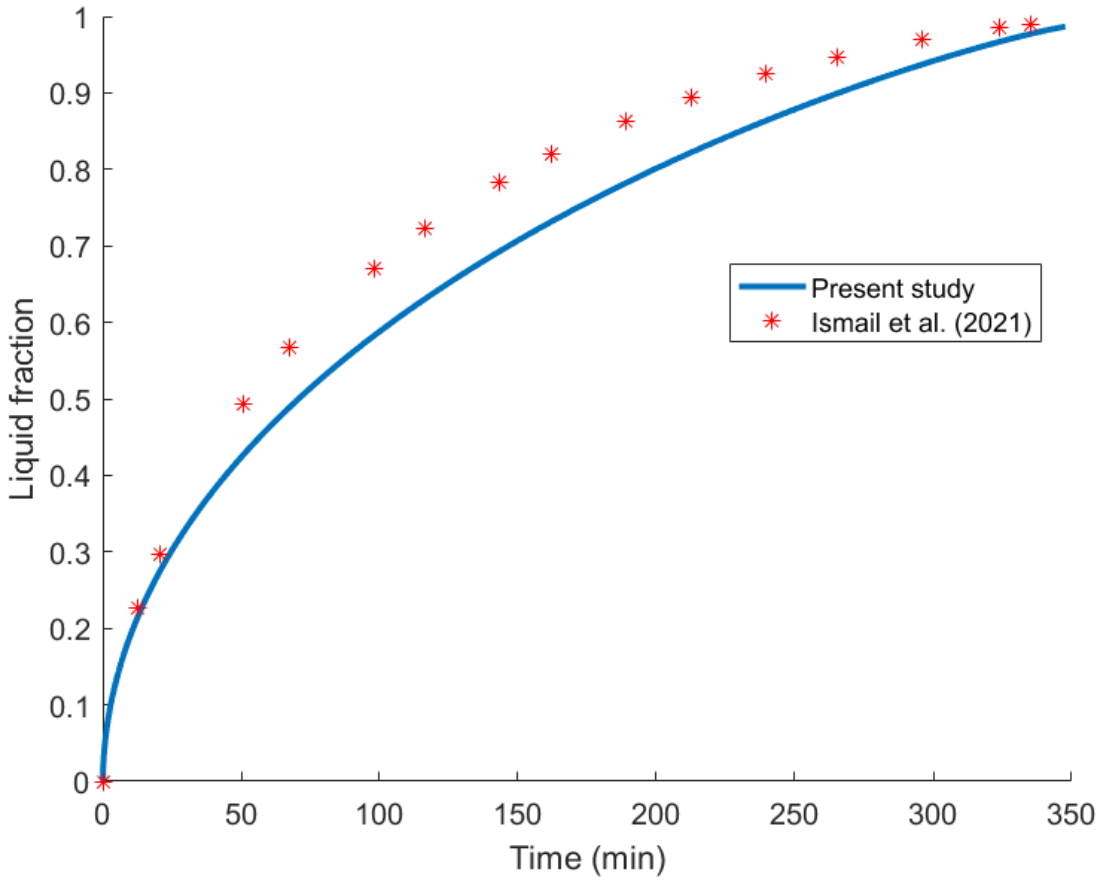

Fig. 3. Comparison between the current computational results and the published data [26] at D = 100 mm, ΔT = 15 K

3. Results and Discussion

The parametric investigation of the influence of air velocity (u_∞), air temperature (T_∞), initial temperature of the PCM (T_{ini}) and PCM diameter (D) on the temperature distribution, phase and liquid fraction is presented in this section. The temperature and phase distributions with time in a 40 mm diameter PCM sphere and T_∞ = 70°C are shown in Figure 4. The centre temperature of the PCM is always lower than the surface temperature (Figure 4(a)). This means that the centre of the PCM is always cooler than the temperature near the surface of the PCM. At t = 45 mins and 60 mins, the temperature contours look almost the same. For higher t, the temperature of the PCM is the same (almost equal to the air temperature) when it reaches steady state after 60 mins (approximately). The diameter of the solid PCM at t = 15 mins was 34 mm and decreased to 30 mm and 20 mm at t = 30 mins and 45 mins respectively (Figure 4(b)). After 75 mins, liquid in entire sphere was observed (not presented here).

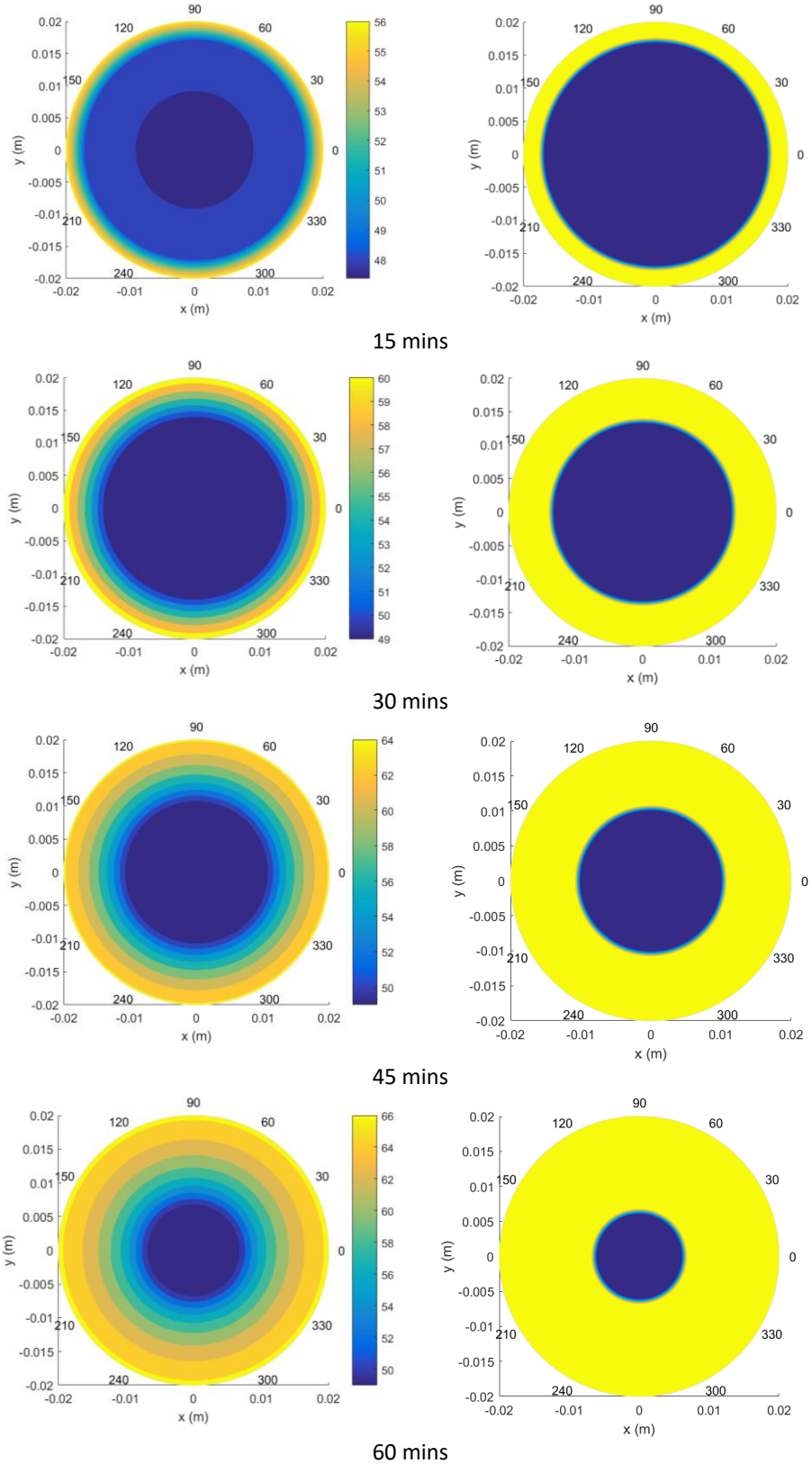

(a) Temperature distribution (b) Phase distribution (yellow: liquid, blue: solid)

Fig. 4. Temperature and phase distributions inside the spherical PCM with D = 40 mm

Figure 5 presents the phase distribution inside a cylinder containing a paraffin wax in a previous work [29]. There is favourable agreement between the current study (Figure 4(b)) and the previous work. In the previous work, water at 73°C temperature was used as the heat transfer fluid.

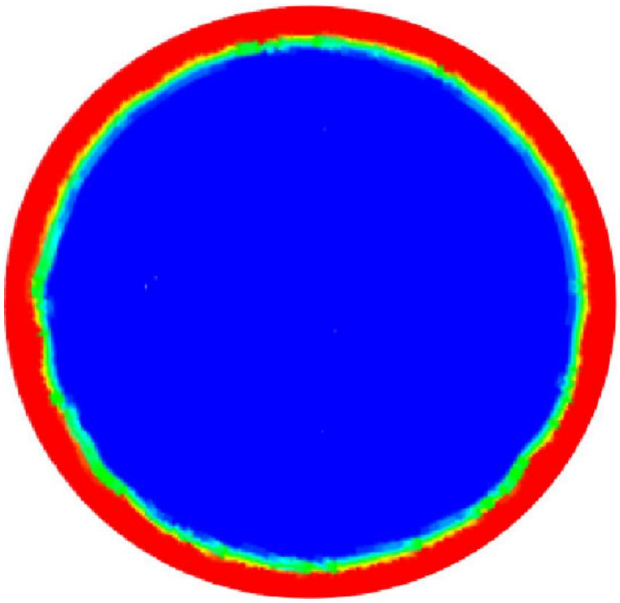

Fig. 5. Phase distribution (red: liquid, blue: solid) inside a cylinder with 26 mm diameter at melting time of 4 mins [29]

Figure 6 shows the liquid fraction versus air velocity in the range of 2 to 5 m/s. Higher hot air velocity generally improves the efficiency of smelting phase change materials by increasing heat transfer rates, reducing the time to complete the phase change and enhancing the uniformity of melting. The PCM heating time without phase change (i.e., liquid fraction = 0) is clearly observed in this figure. It takes about 5 mins to start the melting process. The melting process ends at t = 82 min at air velocity 2 m/s and decreases to 74 mins and 70 mins at velocities 3 m/s and 4 m/s, respectively. As air velocity increases, the thermal boundary layer thickness on the surface of the PCM decreases. A thinner boundary layer enhances heat transfer efficiency, leading to faster melting. The melting time has little change with air velocity because the convective heat transfer coefficient of air is small.

The influence of air temperature on the melting process is evident as shown in Figure 7. As the temperature of the hot air increases, the temperature difference between the hot air and the PCM surface becomes larger. This increases the heat transfer rate, allowing the PCM to absorb heat more quickly and leading to a faster melting process. The melting onset time is 3 mins for T_∞ = 80°C, while at 60°C the melting onset time is 9 mins. After 130 mins, the entire solid PCM is converted to liquid at 60°C. For 80°C, liquefaction takes place in only 52 mins. Higher temperatures result in more rapid energy absorption by the PCM, speeding up the phase transition from solid to liquid.

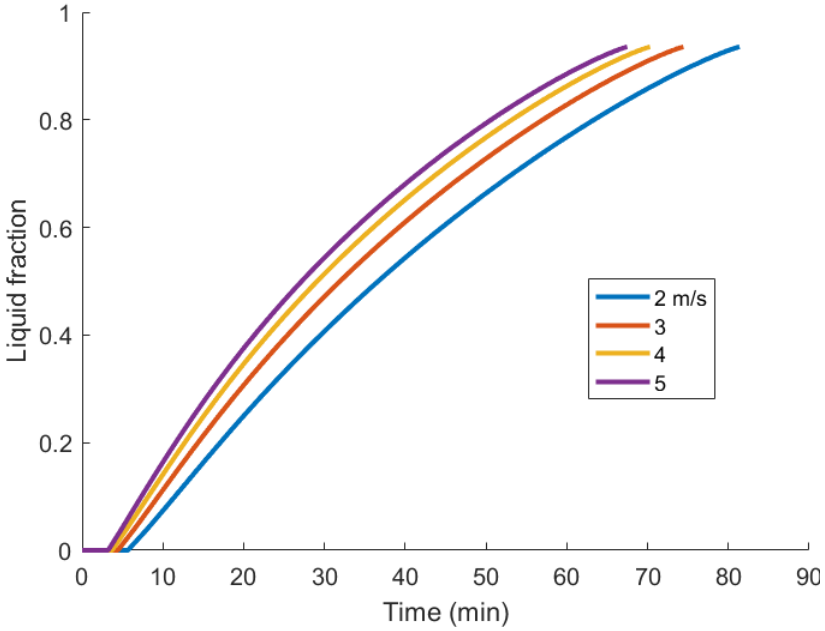

Fig. 6. Effects of air velocity on the liquid fraction

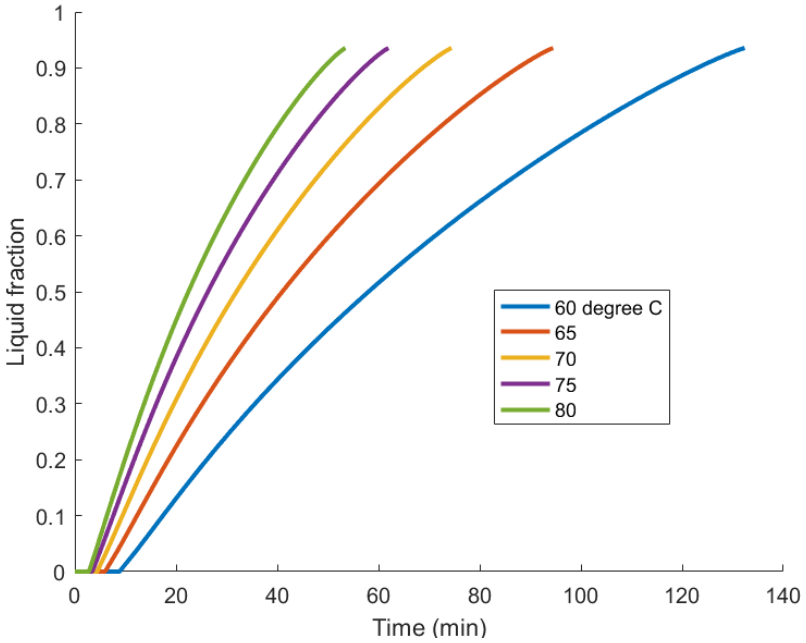

Fig. 7. Liquid fraction at various air temperatures

The effect of initial temperature of PCM on liquefaction is shown in Figure 8. Due to phase change heat transfer, the latent heat transfer is much larger than the sensible heat (very small Stefan number). Therefore, the effect of initial temperature of PCM on melting is negligible. When the initial temperature increases from 30 to 45°C, the time to complete the charging decreases by about 5 mins and the time to start the melting increases by about 3 mins. Higher initial temperatures closer to the melting point reduce energy consumption, speed up the phase change and promote uniform melting. Conversely, lower initial temperatures require more energy and extend melting times.

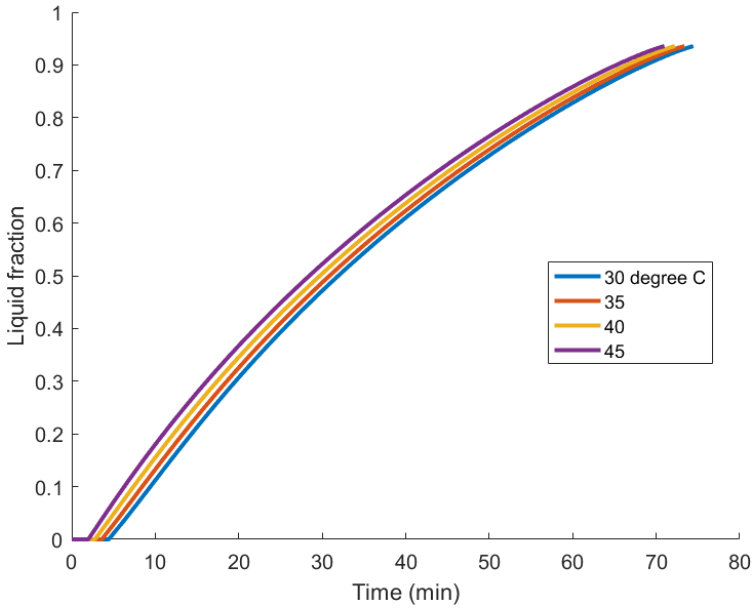

Fig. 8. Liquid fraction at various PCM initial temperatures

The effect of PCM sphere diameter on the liquid fraction is observed in Figure 9. The impact of diameter is obvious because the main heat transfer mechanism in the sphere is conduction. As the diameter increases, thermal resistance increases, thus the melting time increases dramatically. As the diameter increases by 2.5 times, the time to complete the liquefaction increases by 5 times. In other words, as the diameter increases from 40 mm to 100 mm, the melting time increases from 80 mins to 400 mins. When the PCM has a smaller diameter, heat can penetrate the material more quickly due to the shorter distance between the outer surface and the centre. This leads to faster melting because the surface area-to-volume ratio is higher, allowing more efficient heat transfer. A larger PCM diameter results in slower heat transfer because heat must travel a greater distance to reach the core. This creates a lag in melting the inner regions, as the heat initially affects only the outer layers.

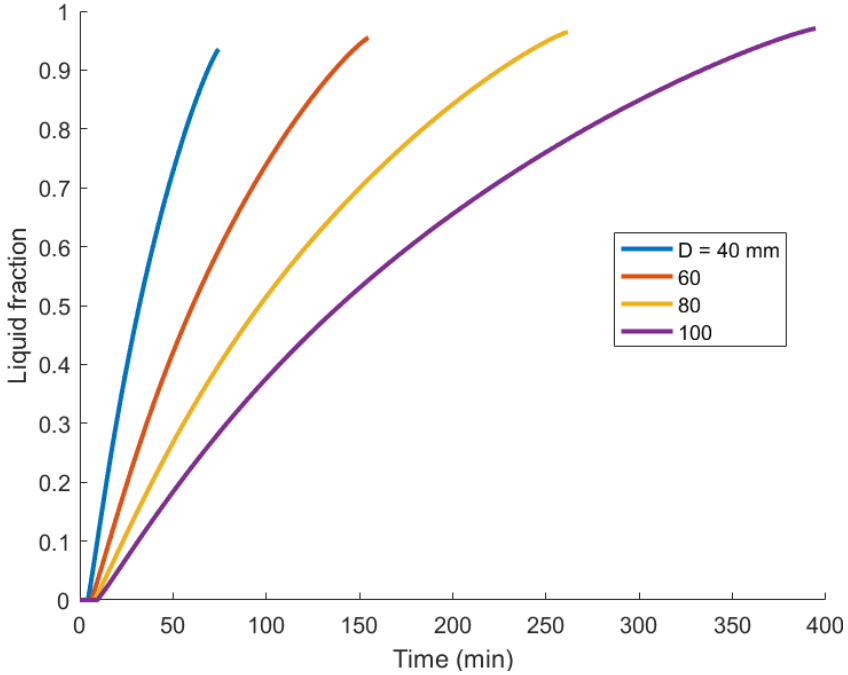

Fig. 9. Liquid fraction at various PCM diameters

4. Conclusions

Numerical investigation of the melting of PCM in a sphere was carried out in this study. The phase change heat transfer was predicted by the enthalpy method. The one-dimensional unsteady energy equation was discretized using the finite difference method. The phase change simulation in this study was validated with published data and achieved good agreement. The phase change problem was formulated towards the heat storage in a solar collector with forced convection of hot air around the sphere. The influence of air velocity, air temperature, PCM diameter and initial temperature of PCM on the temperature and phase distributions and liquid fraction of PCM with time was investigated and analysed. The investigation results showed that the influence of air temperature and the diameter was notable on the melting time of PCM. When the air temperature increased from 60 to 80°C, the melting time of the PCM sphere decreased by 2.5 times. For the increase in sphere diameter from 40 mm to 100 mm, the melting time increases fivefold.

The mathematical model and solution method in this paper can be extended to evaluate the local phase change with respect to the angle of a capsule and the temperature dependence of the air through the collector with respect to the time of day.

Acknowledgement
The author Tran Van Hung acknowledges Ho Chi Minh City University of Technology (HCMUT), VNU-HCM for supporting this study.

References

[1] Sharma, Ashutosh, Ranga Pitchumani and Ranchan Chauhan. "Solar air heating systems with latent heat storage-a review of state-of-the-art." *Journal of Energy Storage* 48 (2022): 104013. https://doi.org/10.1016/j.est.2022.104013

[2] Huang, Lin, Zihao Song, Qichang Dong, Ye Song, Xiaoqing Zhao, Jiacheng Qi and Long Shi. "Surface temperature and power generation efficiency of PV arrays with various row spacings: A full-scale outdoor experimental study." *Applied Energy* 367 (2024): 123362. https://doi.org/10.1016/j.apenergy.2024.123362

[3] Phu, Nguyen Minh, Lai Hoai Nam and Nguyen Le Hong Son. "Unsteady analysis of a solar air heater with sensible heat storage using 2D finite difference approximation." *Journal of Mechanical Science and Technology* 37, no. 11 (2023): 6019-6028. https://doi.org/10.1007/s12206-023-1038-9

[4] Jain, Dilip. "Modeling the system performance of multi-tray crop drying using an inclined multi-pass solar air heater with in-built thermal storage." *Journal of food engineering* 71, no. 1 (2005): 44-54. https://doi.org/10.1016/j.jfoodeng.2004.10.016

[5] Das, Pritam and Chandramohan VP. "Performance characteristics of divergent chimney solar updraft tower plant." *International Journal of Energy Research* 45, no. 12 (2021): 17159-17174. https://doi.org/10.1002/er.5304

[6] Azmi, Mohd Irwan Mohd, Nor Azwadi Che Sidik, Yutaka Asako, Wan Mohd Arif Aziz Japar, Nura Muaz Muhammad and Nadlene Razali. "Numerical Studies on PCM Phase Change Performance in Bricks for Energy-Efficient Building Application–A Review." *Journal of Advanced Research in Numerical Heat Transfer* 1, no. 1 (2020): 13-21.

[7] Kean, Tung Hao, Nor Azwadi Che Sidik, Yutaka Asako, Tan Lit Ken and Siti Rahmah Aid. "Numerical study on heat transfer performance enhancement of phase change material by nanoparticles: a review." *Journal of Advanced Research in Fluid Mechanics and Thermal Sciences* 45, no. 1 (2018): 55-63.

[8] Hedau, Ankush and S. K. Singal. "Study on the thermal performance of double pass solar air heater with PCM-based thermal energy storage system." *Journal of Energy Storage* 73 (2023): 109018. https://doi.org/10.1016/j.est.2023.109018

[9] Rahim, Nasrullah Che, Muhammad Fairuz Remeli, Baljit Singh and Hazim Moria. "Designing a Solar Heat Storage System using Heat Pipe and Phase-Change Material (PCM)." *Journal of Advanced Research in Fluid Mechanics and Thermal Sciences* 91, no. 1 (2022): 102-114. https://doi.org/10.37934/arfmts.91.1.102114

[10] Phu, Nguyen Minh and Nguyen Thanh Luan. "A review of energy and exergy analyses of a roughened solar air heater." *Journal of Advanced Research in Fluid Mechanics and Thermal Sciences* 77, no. 2 (2021): 160-175. https://doi.org/10.37934/arfmts.77.2.160175

[11] Hai, Doan Thi Hong and Nguyen Minh Phu. "A critical review of all mathematical models developed for solar air heater analysis." *Journal of Advanced Research in Fluid Mechanics and Thermal Sciences* 105, no. 1 (2023): 1-14. https://doi.org/10.37934/arfmts.105.1.114
[12] Román, Franz, Zeeshan Munir and Oliver Hensel. "Performance comparison of a fixed-bed solar grain dryer with and without latent heat storage." *Energy Conversion and Management: X* 22 (2024): 100600. https://doi.org/10.1016/j.ecmx.2024.100600
[13] Yadav, Satyapal, Abhay Bhanudas Lingayat, V. P. Chandramohan and V. R. K. Raju. "Numerical analysis on thermal energy storage device to improve the drying time of indirect type solar dryer." *Heat and Mass Transfer* 54 (2018): 3631-3646. https://doi.org/10.1007/s00231-018-2390-7
[14] Bouadila, Salwa, Sami Kooli, Mariem Lazaar, Safa Skouri and Abdelhamid Farhat. "Performance of a new solar air heater with packed-bed latent storage energy for nocturnal use." *Applied Energy* 110 (2013): 267-275. https://doi.org/10.1016/j.apenergy.2013.04.062
[15] Bouadila, Salwa, Mariem Lazaar, Safa Skouri, Sami Kooli and Abdelhamid Farhat. "Energy and exergy analysis of a new solar air heater with latent storage energy." *international journal of hydrogen energy* 39, no. 27 (2014): 15266-15274. https://doi.org/10.1016/j.ijhydene.2014.04.074
[16] Arfaoui, Nessim, Salwa Bouadila and Amenallah Guizani. "A highly efficient solution of off-sunshine solar air heating using two packed beds of latent storage energy." *Solar Energy* 155 (2017): 1243-1253. https://doi.org/10.1016/j.solener.2017.07.075
[17] Sudhakar, P. and M. Cheralathan. "Encapsulated PCM based double pass solar air heater: A comparative experimental study." *Chemical Engineering Communications* 208, no. 6 (2021): 788-800. https://doi.org/10.1080/00986445.2019.1641701
[18] Verma, Geeta and Satyender Singh. "Computational multiphase iterative solution procedure for thermal performance investigation of phase change material embedded parallel flow solar air heater." *Journal of Energy Storage* 39 (2021): 102642. https://doi.org/10.1016/j.est.2021.102642
[19] Cengel, Yunus, John Cimbala and Robert Turner. *EBOOK: Fundamentals of Thermal-Fluid Sciences (SI units)*. McGraw Hill, 2012.
[20] Ture, Saurabh Avinash and V. P. Chandramohan. "Effect of radiation heat transfer in convective drying of cranberry: Numerical solutions of one and two dimensional heat and mass transfer and comparison of results." *Thermal Science and Engineering Progress* 22 (2021): 100837. https://doi.org/10.1016/j.tsep.2020.100837
[21] Goyal, Mukul Kumar, Saurabh Avinash Ture and V. P. Chandramohan. "Effect of shrinkage in convective drying of spherical food material: A numerical solution." *Arabian Journal for Science and Engineering* 46, no. 12 (2021): 12283-12298. https://doi.org/10.1007/s13369-021-05957-1
[22] Arunsandeep, G., Abhay Lingayat, V. P. Chandramohan, V. R. K. Raju and K. Srinivas Reddy. "A numerical model for drying of spherical object in an indirect type solar dryer and estimating the drying time at different moisture level and air temperature." *International Journal of Green Energy* 15, no. 3 (2018): 189-200. https://doi.org/10.1080/15435075.2018.1433181
[23] Ellendt, N., A. M. Lumanglas, S. Imani Moqadam and L. Mädler. "A model for the drag and heat transfer of spheres in the laminar regime at high temperature differences." *International Journal of Thermal Sciences* 133 (2018): 98-105. https://doi.org/10.1016/j.ijthermalsci.2018.07.009
[24] Klein, Sanford A. and Gregory Nellis. *Mastering ees*. Madison, WI, USA: f-Chart software, 2013.
[25] Reddy, K. S. "Thermal modeling of PCM-based solar integrated collector storage water heating system." (2007): 458-464. https://doi.org/10.1115/1.2770753
[26] Ismail, Mohammad, Awni H. Alkhazaleh, Jafar Masri, Abdullah Masoud Ali and Malek Ali. "Experimental and numerical analysis of paraffin waxes during solidification inside spherical capsules." *Thermal Science and Engineering Progress* 26 (2021): 101095. https://doi.org/10.1016/j.tsep.2021.101095
[27] Lee, Huei-Huang. *Programming with MATLAB 2016*. SDC Publications, 2016.
[28] Özişik, M. Necati, Helcio RB Orlande, Marcelo J. Colaço and Renato M. Cotta. *Finite difference methods in heat transfer*. CRC press, 2017. https://doi.org/10.1201/9781315168784
[29] Shaker, Mohammad Yaseen, Ahmed A. Sultan, Emad A. El Negiry and Ali Radwan. "Melting and solidification characteristics of cylindrical encapsulated phase change materials." *Journal of Energy Storage* 43 (2021): 103104. https://doi.org/10.1016/j.est.2021.103104